PERGAMON

Atmospheric Environment 35 (2001) 6151–6165

ATMOSPHERIC ENVIRONMENT

www.elsevier.com/locate/atmosenv

Modeling biogenic emissions of isoprene: exploration of model drivers, climate control algorithms, and use of global satellite observations

Christopher S. Potter[a,*], Susan E. Alexander[b], Joseph C. Coughlan[a], Steven A. Klooster[b]

[a] *NASA Ames Research Center, Moffett Field, CA 94035, USA*
[b] *California State University Monterey Bay, Seaside, CA 93955, USA*

Received 12 March 2001; received in revised form 28 June 2001; accepted 20 July 2001

Abstract

An improved global budget for isoprene emissions from terrestrial vegetation sources is fundamental to a better understanding of the oxidative capacity of the lower atmosphere and changes in the concentration of major greenhouse gases. In this study, we present a biosphere modeling analysis designed to ascertain the interactions of global data drivers for estimating biogenic isoprene emissions. We have integrated generalized isoprene emission algorithms into a process-based simulation model of ecosystem carbon fluxes, the NASA-CASA (Carnegie–Ames–Stanford Approach) model. This new modeling approach for predicting isoprene emissions operates on scales designed to directly link regional and global satellite data sets with estimates of ecosystem carbon cycling, hydrology, and related biogeochemistry. The NASA-CASA model results indicate that the annual isoprene flux from terrestrial plant sources is 559 Tg C. Three ecosystem types, broadleaf evergreen forest, dry tropical forest, and wooded grassland (savanna), account for approximately 80% of these global vegetation isoprene emissions. Based on analyses to improve understanding of the relative influence of climatic (e.g., light and temperature) versus biotic (NPP) controllers on predicted isoprene emission estimates, it appears that the largest portion of total biogenic flux to the global atmosphere is emitted from ecosystems that are mainly light-limited for isoprene emissions. These modeling results imply that, along with better process understanding of base emission factor controls for volatile organic compounds, improvements in global fields of solar surface radiation fluxes in warm climate zones will be needed to reduce major uncertainties in isoprene source fluxes.

Keywords: Isoprene; Biogenic emissions; Remote sensing; Ecosystem modeling; Emission factors

1. Introduction

Isoprene (2-methyl 1,3-butadiene), a volatile organic compound (VOC) emitted from predominately natural sources, has an important impact on atmospheric chemistry and air quality. Global emissions of isoprene from vegetation are estimated at approximately 500 Tg (10^{12} g) C yr^{-1}, and comprise the primary source of photochemically reactive, reduced trace gases in the troposphere (Guenther et al., 1995). This terrestrial biogenic source of isoprene is an emission flux comparable to the sum of anthropogenic methane (CH_4) emissions plus biogenic sources of CH_4. Isoprene emission also represents a significant loss of carbon from certain higher plants (Lerdau and Throop, 1999). Although field surveys and laboratory studies indicate high variability in VOC fluxes among different types of plants, emissions from forested regions, especially those

*Corresponding author. Tel.: +1-650-604-6164; fax: +1-650-604-4680.
E-mail address: cpotter@gaia.arc.nasa.gov (C.S. Potter).

1352-2310/01/$ - see front matter
PII: S1352-2310(01)00390-9

in tropical ecosystems, are apparently the largest source of isoprene to the atmosphere (Rasmussen and Khalil, 1988; Fehsenfeld et al., 1992, Guenther et al., 1995; Lerdau and Keller, 1997).

There is considerable interest in obtaining more accurate isoprene emission estimates, particularly because isoprene plays an important role in regulating the oxidative capacity of the lower atmosphere and influencing the concentration of greenhouse gases. Isoprene reacts rapidly with the hydroxyl radical (OH), the principal oxidizing compound of the troposphere, and indirectly affects climate forcing by influencing the concentrations of carbon monoxide, ozone, and methane (Fehsenfeld et al., 1992). Isoprene is also considerably more reactive with OH than is methane, reducing the concentration of OH in the atmosphere and potentially increasing the atmospheric lifetime (and strength as a greenhouse gas) of CH_4 (Jacob and Wofsy, 1988).

Although there is still uncertainty in terms of biotic regulation mechanisms, plants potentially emit isoprene as a means of thermal protection of thylakoid membranes within chloroplasts (Sharkey and Singsaas, 1995). This observation of higher heat tolerance among (non-desert) plant species that emit more isoprene has been made in investigations of the theory that isoprene fluxes correlate closely with changes in leaf temperature, and possibly moisture stress, throughout the course of a warm day (Singsaas and Sharkey, 2000). Supporting evidence comes from studies of shaded foliage that emits almost no isoprene, but which can be induced to emit increasing amounts after exposure to high light and temperature conditions (Guenther et al., 1999). If proven correct, the thermal protection theory has important implications for air quality, because the highest rates of biogenic isoprene emissions would likely occur on hot, still days when there is the potential for development of high levels of tropospheric ozone in locally polluted air. Rates of ozone generation are complex, and maybe non-linearly dependent upon the concentrations of various hydrocarbons present (Chameides and Lodge, 1992). Isoprene emissions can also represent a significant loss of carbon from forest ecosystems, often in the range of 0.5–3% of net plant photosynthesis, possibly increasing to over 10% under conditions of temperature or moisture stress (Sharkey et al., 1991; Monson and Fall, 1989).

Current regional and global models of isoprene emission are based principally on ecosystem-specific biomass density and base VOC emission factor estimates, linked to control algorithms describing the relationship between light, temperature, and isoprene emission in plant canopies (Turner et al., 1991; Guenther et al., 1995, 1999; Lamb et al., 1996; Constable et al., 1999; Zimmer et al., 2000). Large uncertainties exist, however, in both the base emission factor values and the climate control algorithms for such models. For example, ecological adaptations may account for the observation that tropical plants show a different relationship between light intensity and isoprene emissions than do temperate plant species (Lerdau and Keller, 1997; Guenther, 1999). Furthermore, although there is some evidence that isoprene emission fluxes may be coupled metabolically to leaf photosynthesis rates (Monson et al., 1991; Lerdau and Throop, 1999), experimental field studies have yet to conclusively establish whether base (standard temperature and irradiance) isoprene emission rates can scale effectively with short-term (e.g., hourly) rates of net carbon assimilation. Neither is it known with certainty if there is a consistent percentage of high isoprene-emitting plant taxa across many different ecosystem types.

In this study, we present an analysis aimed at exploring new modeling approaches and the importance of different global data drivers for estimating biogenic isoprene emissions. Our long-term study objectives are to: (1) develop linkages between a generalized VOC emission algorithm and a process-based simulation model of ecosystem carbon fluxes, the NASA-CASA (Carnegie–Ames–Stanford Approach) model (Potter et al., 1999), which operates on scales designed to link regional and global satellite data sets with estimates of ecosystem production, hydrology, and biogeochemistry; (2) understand the relative importance of various global model drivers, climate control algorithms, and base VOC emission rates in this coupled biogenic isoprene emission-terrestrial ecosystem framework; and (3) evaluate the requirements for addition of hourly canopy level photosynthesis and stomatal conductance control algorithms to the NASA-CASA VOC model for more precise regulation of leaf temperature, carbon assimilation rates, and potential moisture stress on predictions of the diurnal cycle for isoprene emission fluxes.

A chief advantage of linking VOC emission algorithms successfully with a model like NASA-CASA is the ability to use satellite-derived images of vegetation canopy properties, such as leaf area coverage, also called 'greenness' cover, and foliar biomass density. The detailed temporal and spatial patterns in ecosystem cover recorded by global observing satellite sensors can provide classifications of ecosystem types with distinctive seasonal trends in phenology (e.g., onset, peak, and duration of canopy greenness), which are closely related to rates of total carbon assimilation and possibly to VOC emissions (Guenther et al., 1999). Regular updates of land surface conditions and vegetation properties observed from NASA's new Terra satellites (Knyazikhin et al., 1998) will be used in future years to drive the NASA-CASA production and coupled VOC model at regional and global scales.

2. Modeling approach

In this section, we present a new satellite-driven modeling approach to explore biogenic isoprene emissions. Our modeling approach, similar in many ways to an existing modeling framework for VOC emissions presented by Guenther et al. (1995), is unique in using outputs from the well-tested NASA-CASA model for terrestrial ecosystem production (Potter et al., 1999), as well as satellite-derived ecosystem classification (DeFries et al., 1994, 1995) and a satellite vegetation index (Los et al., 1994), as drivers of global biogenic isoprene emissions. The resulting VOC emissions products from the global coverage at 1° spatial resolution provided by the satellite data sets should enable direct linkage to atmospheric models of trace gas transport. To our knowledge, no other VOC emission model to date has been applied using global satellite inputs to extrapolate isoprene fluxes over all terrestrial ecosystem types. Recent regional modeling studies for isoprene have used satellite data products for defining relatively small-scale land cover distributions (Guenther et al., 1999), an approach also possible using the version of NASA-CASA applied at 8-km spatial resolution (Potter et al., 1998).

2.1. Terrestrial carbon cycling

The NASA-CASA (Carnegie–Ames–Stanford)–Biosphere model is a representation of daily and monthly fluxes of water, carbon, and nitrogen in terrestrial ecosystems, using inputs of global satellite observations for land surface properties and climate drivers for predictions of terrestrial biogeochemical cycling (Potter, 1997; Potter et al., 1999). The model is designed to simulate seasonal patterns in net carbon fixation and allocation, litterfall, and soil nutrient mineralization, and soil CO_2 emissions. Our fundamental approach to estimating net primary production (NPP) is to define optimal metabolic rates for major biogeochemical processes, and adjust these spatially uniform variables using unitless scalars related to the limiting effects of solar radiation, air temperature, predicted soil moisture, litter substrate quality (nitrogen and lignin contents), soil texture, and land use. Carbon (CO_2) fixed by vegetation is estimated in the model according to the amount of photosynthetically active radiation (PAR; W m^{-2}) intercepted by plant canopies and converted to plant biomass. NPP is calculated in grams of carbon fixed per day or per month. In validation analyses using measured NPP estimates from thousands of ecosystem sites through the world, we find that NASA-CASA predicts annual NPP with an overall error of less than 10% (unpublished data).

For application in this study, several other model components of NASA-CASA version described by Potter et al. (1999) remain unchanged. For example, the daily or monthly fraction of overstory NPP, defined as net fixation of CO_2 by vegetation, is computed on the basis of light-use efficiency (Monteith, 1972). Production of new plant biomass is estimated as a product of surface irradiance flux, S_r in W m^{-2}, the unitless fraction of absorbed PAR (FPAR), and a light utilization efficiency term (ε_{max}) that is modified by air temperature (T_a) and soil moisture (W) unitless stress scalars (Eq. (1)).

$$\mathrm{NPP} = S_r\,\mathrm{FPAR}\,\varepsilon_{max}\,T_a\,W \quad (1)$$

The ε_{max} term is set uniformly at 0.56 g C MJ^{-1} PAR, a value that derives from calibration of predicted annual NPP to previous field estimates of NPP (Potter et al., 1993). The T_a stress term is computed with reference to derivation of optimal temperatures (T_{opt}) for plant production. The T_{opt} setting will vary by latitude and longitude, ranging from near 0°C in the Arctic to the middle thirties in low latitude deserts. The W term is estimated from monthly water deficits, based on a comparison of moisture supply (precipitation and stored soil water) to demand potential evapotranspiration (PET) using the method of Thornthwaite (1948). Freeze-thaw dynamics with soil depth operate according to the degree-day method of Jumikis (1966), as described by Bonan (1989).

Estimates of FPAR are derived using a normalized difference vegetation index (NDVI). NDVI is a unitless parameter (scaled from 0 to 1000) computed from the ratio of visible and near infra-red radiation channels. Global coverage of NDVI can be obtained from the advanced very high resolution (AVHRR) satellite sensor as this channel ratio. The AVHRR NDVI greenness has been closely correlated with vegetation parameters such as FPAR at coarse spatial resolutions of 1° latitude–longitude (Running and Nemani, 1988; Sellers et al., 1994; DeFries et al., 1995). The use of FPAR and NPP for predicting foliar density differs from the use of a global vegetation index (GVI) by Guenther et al. (1995), in that FPAR is a relatively well-calibrated and validated parameter for vegetation canopies (Sellers et al., 1994, 1995), unlike the GVI for estimating foliar density over large areas of the land surface.

2.2. Isoprene emission algorithm

The isoprene emission portion of our model is based on the international global atmospheric chemistry (IGAC) program's global hydrocarbon emission framework, similar to the model described by Guenther et al. (1995). The general emission algorithm is common among existing biosphere VOC models (Guenther, 1999; Eq. (2)), and has been used mainly to estimate isoprene emissions from plant canopies:

$$F = f\,(\mathrm{Fd})\,f\,(Q)\,f\,(T)\,f\,(G)\,\varepsilon_v\,\rho \quad (2)$$

where F is the VOC emission flux, modeled as a function of foliar density (Fd; g dry matter m^{-2}), and unitless scalars for solar irradiance effect (Q), leaf temperature effect (T), plant growth stage effect (G), a plant-specific base emission rate (ε_v; at PAR flux of 1000 μmol m^{-2} s^{-1} and leaf temperature of 303.15 K), and the escape efficiency of VOC to the above-canopy air mass (ρ).

The minimum set of input data sets necessary for calculating global isoprene fluxes include gridded surface air temperature, solar radiation flux, net primary production (NPP), and ecosystem type. Satellite remote sensing data can be used to help compute each of these inputs to the Fd, $f(Q)$, and $f(G)$ terms in this general equation for VOC emissions. More information on global data drivers is provided in a following section of the paper.

Foliar density is computed according to the following equation:

$$\mathrm{Fd} = \mathrm{Fr}\,\mathrm{NPP}\,e^{(\ln(2)((G-G')/G_{\max}-G'))-1)} \quad (3)$$

where Fr is an ecosystem-dependent empirical coefficient (Box, 1981), NPP is computed from the NASA-CASA model (Potter et al., 1999), G is a monthly global vegetation cover index equal to 10^2 (1 + NDVI), $G_{\max}$ is the highest monthly estimate of G during the year, and G' is a constant set equal to 110 for wooded ecosystems and 102 for all other ecosystems.

As developed by Guenther et al. (1995), a simple canopy radiative transfer model, described originally by Norman (1982), is used for our CASA VOC model to compute fluxes of absorbed PAR in the leaf profile. These results serve as input to the $f(Q)$ term in Eq. (2). Above-canopy conditions for temperature are adjusted as a function of canopy position (sunlit or shaded leaves). Leaf-sun angles are computed for estimates of cloud-corrected solar radiation reaching both groups of sunlit and shaded leaves in the canopy. The sunlit and shaded (f_{sun} and f_{shade}) portions of the canopy leaf area index (LAI, m^2 m^{-2}) are estimated as

$$\mathrm{LAI} = \mathrm{Fd}/\mathrm{SLW}, \quad (4)$$

$$\mathrm{LAI}_{\mathrm{sun}} = \mathrm{LAI}[1 - e^{(-0.5\,\mathrm{LAI}/\sin(B))}]\sin(B)/\cos(A), \quad (5)$$

$$\mathrm{LAI}_{\mathrm{shade}} = \mathrm{LAI} - f_{\mathrm{sun}}, \quad (6)$$

$$\mathrm{PAR}_{\mathrm{sun}} = \mathrm{PAR}_{\mathrm{dir}}\cos(A)/\sin(B) + \mathrm{PAR}_{\mathrm{shade}}, \quad (7)$$

$$\mathrm{PAR}_{\mathrm{shade}} = \mathrm{PAR}_{\mathrm{diff}}\,e^{(-0.5\,\mathrm{LAI}^{0.7})} + \mathrm{PAR}_1, \quad (8)$$

$$\mathrm{PAR}_1 = 0.07\,\mathrm{PAR}_{\mathrm{dir}}\,(0.1 - 0.1\,\mathrm{LAI})\,e^{(-\sin(B)} \quad \text{for } \mathrm{LAI} < 1; 0 \text{ for } \mathrm{LAI} \geqslant 1, \quad (9)$$

where SLW is the specific leaf weight (g m^{-2}; Box, 1981), A is the mean leaf-sun angle and B is the solar elevation angle (both from Iqbal, 1983), $\mathrm{PAR}_{\mathrm{dir}}$ is flux of direct PAR above the canopy, $\mathrm{PAR}_{\mathrm{diff}}$ is flux of diffuse PAR above the canopy, and PAR_1 is flux from multiple scattering of direct beam radiation. As described above, monthly values for total canopy maximum seasonal foliar density are computed from the NASA-CASA model's NPP algorithms (Potter et al., 1993), with conversion factors for peak foliar mass set according to ecosystem types in the land cover classification system from DeFries and Townshend (1994), shown in Fig. 1.

Functional response algorithms used to estimate the controls by light and temperature on plant isoprene emissions are the same as those described by Guenther et al. (1991, 1995). The $f(Q)$ response is a saturating function of PAR (μmol m^{-2} s^{-1}), whereas $f(T)$ is an exponential function of leaf temperature (K), both used to compute normalized controller terms (Fig. 2) for Eq. (2). Controller values near 1.0 represent low limitation of light or temperature on VOC emission rates, while values of zero represent the complete limitation of VOC emission rates. There is some evidence that the $f(T)$ should incorporate the past several days or weeks of temperature conditions to which foliage has been exposed (Sharkey et al., 1999), and our use of monthly average temperature drivers for this global study may capture this effect to some extent. If instead rapid daily changes in temperature have more important non-linear effects on VOC emission (Geron et al., 2000), the use of monthly model inputs would not readily capture these controls.

Lacking more definitive information, base emission factors (ε_v) for isoprene are defined in the same manner as those reported by Guenther et al. (1995) according to ecosystem types in Olson's (1992) global ecosystem classification (Table 1). We translated these groupings from on Olson's map system into the satellite-based land cover classification system from DeFries et al. (1994), in order to reduce the number of ecosystem classes to a level compatible with the NASA-CASA model framework. The satellite-derived classification map of DeFries et al. (1994) may decrease the model precision somewhat by decreasing the number of ecosystem cover types globally, but because of the reliable classification techniques based on seasonal patterns of NDVI, it has a potential to improve accuracy within those cover types over more traditional vegetation maps.

Beyond the emission factor estimates from Guenther et al. (1995), Lerdau and Keller (1997) have demonstrated the potential importance of seasonally dry (drought-deciduous) tropical forests to regional VOC emissions. Hence, we added a distinct dry tropical forest (DTF) class to NASA-CASA land cover scheme for VOC emissions. Areas of DTF were delineated within the general evergreen tropical forest class of DeFries et al. (1994) as those locations where climatology records from Leemans and Cramer (1990) show three or more months with rainfall totals of <4.5 cm (Potter et al., 1998).

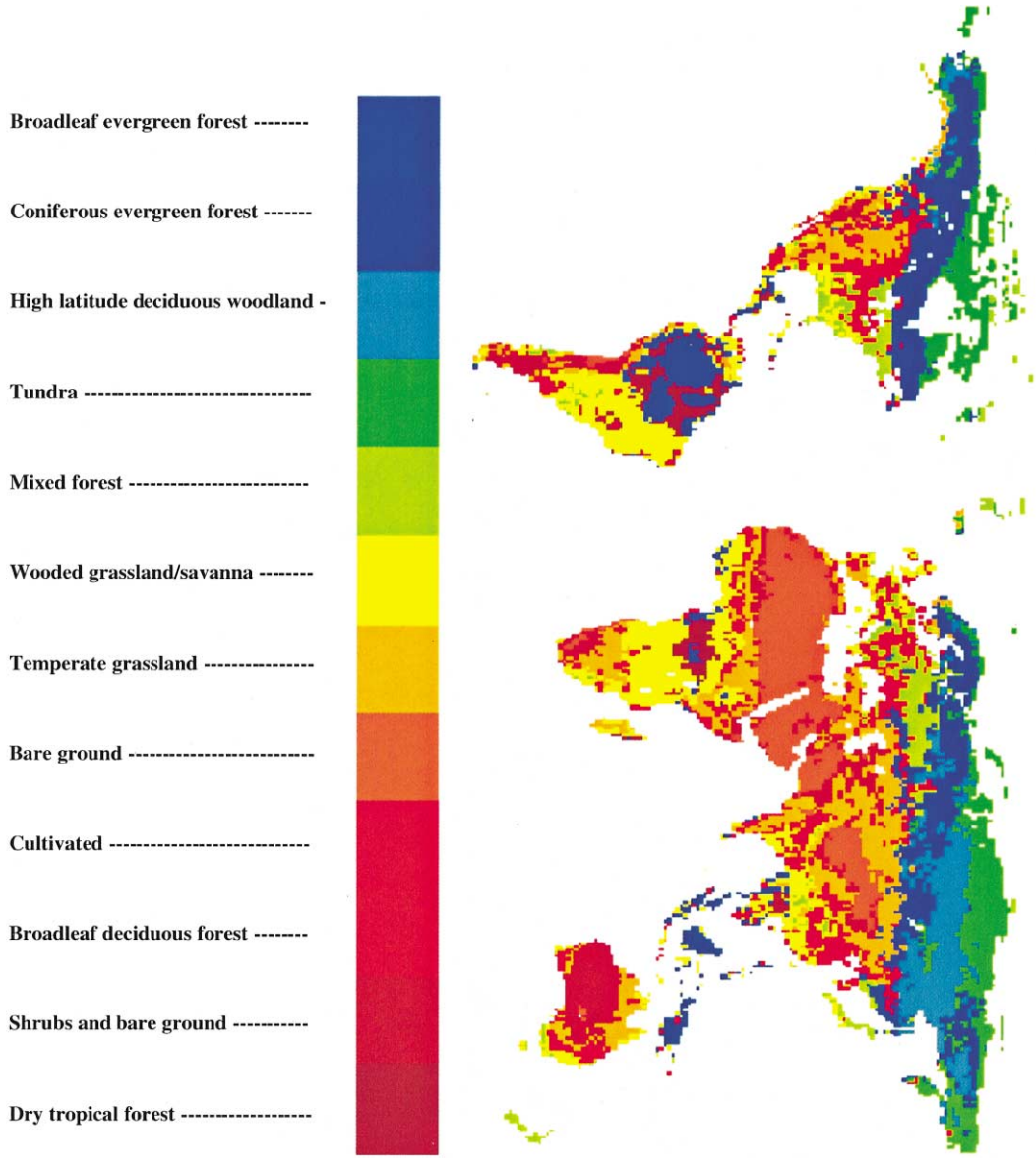

Fig. 1. Ecosystem cover types used in the NASA-CASA model for VOC emissions (source: DeFries and Townshend, 1994).

The $f(G)$ term can be used in Eq. (2) to add an effect of plant growth stage from seedling to mature plant. In our global application for isoprene emissions, we set the (G) term to a uniform value of unity, lacking more specific growth stage information in terms of plant age structure from every global land cover pixel. We have already included the effect of early season leaf expansion and yearly phenology in this equation through the use of NDVI remote sensing inputs, which control changes each month in foliar density. In terms of sensitivity, it is pointed out by Guenther et al. (1999) that inclusion of a model term to account for changes in leaf age across years and seasonal phenology patterns can result in a 16% decrease in estimated VOC emissions at regional scales.

In the absence of comprehensive information from field measurements, the escape efficiency of VOC to the above-canopy air mass is assumed to be globally uniform at a value of $\rho = 1.0$. We note, however, that Guenther et al. (1999) report inclusion of a locally estimated ρ term could result in an additional 5% decrease in estimated VOC emissions. Therefore, it is

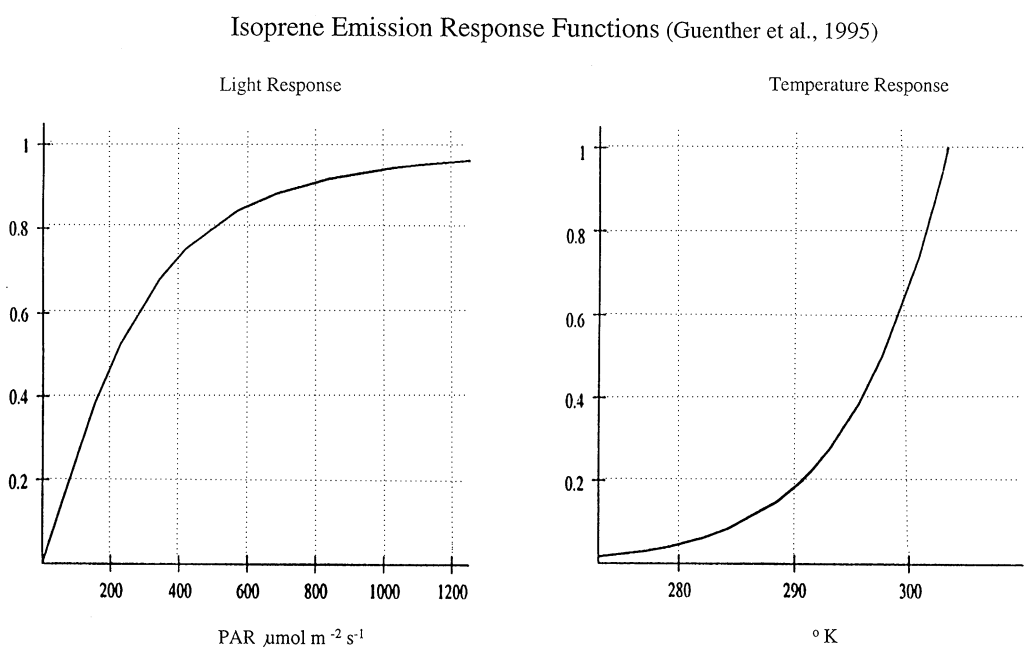

Fig. 2. Functional response algorithms for the controls by light and temperature on plant isoprene emissions.

important to clarify that Eq. (2) used in our study is an estimate of emission flux prior to (re)entrainment of isoprene by vegetation canopies.

2.3. Global data drivers

As global climate drivers for our CASA VOC emission model, monthly mean surface temperature and precipitation were based on long-term (1931–1960) average values at 1° spatial resolution (Leemans and Cramer, 1990). Cloud-corrected surface solar irradiance data were obtained from the SeaWiFS (Sea-viewing Wide Field-of-view Sensor) radiation flux estimates of Bishop and Rossow (1991). These estimates for PAR fluxes are derived as a product of the International Satellite Cloud Climatology Project (ISCCP) and gridded originally at a spatial resolution of 2.5° for the period July 1983 to June 1991. These PAR flux data are documented to have an accuracy of 9 W m^{-2} on a daily basis and less than 4% overall bias in the 17-day mean relative to ground measurements.

For derivation of FPAR at 1° spatial resolution, complete AVHRR data sets for the 1980s have been produced from National Atmospheric and Oceanic Administration (NOAA) Global Area Coverage (GAC) Level 1B data. These data consist of reflectances and brightness temperatures derived from the five-channel cross-track scanning AVHRR aboard the NOAA Polar Orbiter 'afternoon' satellites (NOAA-7, -9, -11, and -14). Monthly composite NDVI data sets remove much of the contamination due to cloud cover present in the daily AVHRR data (Holben, 1986). Additional processing of the satellite imagery is necessary nevertheless to eliminate remaining artifacts. As part of the Global Inventory Monitoring and Modeling Studies (GIMMS) program (Los et al., 1994) of NASA Goddard Space Flight Center, Sellers et al. (1994) developed Fourier algorithms (FA) and solar zenith (S) angle adjustments for interannual AVHRR data sets to further correct NDVI signals from global 1° data sets (averaged from 8-km values) for the 1980s. FAS processing appears to remove many artifacts present in previous NDVI data sets, including cloud cover and aerosol interference. These GIMMS NDVI data show minimal correlations with equatorial crossing times of the NOAA satellites (Malmström et al., 1997), which suggests that corrections have been made for orbital drifts and switches between satellites (e.g., NOAA-9 to NOAA-11).

In up-scaling from the leaf to the canopy level to extrapolate leaf temperature profiles, carbon assimilation rates, and other effects on plant VOC emissions, it is advantageous to utilize the strong correlation between FPAR and the simple ratio (SR) of near-infrared reflectance to visible reflectance from vegetated surfaces. The SR is recorded by coarse resolution (1-km) satellite sensors and used already in the NASA-CASA model (this study). Sellers et al. (1995), for example, have described the strong linear relationship between canopy level rates of carbon assimilation (A_C) and conductance

Table 1
Base emission rate (ε_v) categories for isoprene (Guenther et al., 1995), following ecosystem classification system from Olson (1992)

Emission rate = 5 μg C g^{-1} h^{-1}: Total area: 15.79 (12.02%)
30 Farm/city—cool (2.91)
31 Farm/city—warm (8.94)
36 Paddy rice (1.98)
37 Irrigated crop—warm (1.28)
64 Heath/moorland (0.16)
72 African swamp (0.16)
Other crops/grass (0.36)
Emission rate = 8 μg C g^{-1} h^{-1}: Total area: 19.95 (15.18%)
20 Snow/rain conifers (0.16)
22 Snowy conifers (2.83)
21 Boreal conifers (5.24)
23 Snowy mixed (1.53)
44 Bog (1.04)
45 Marsh/swamp (1.67)
58 Crops/woods—warm (2.97)
62 Maritime taiga (4.51)
Emission rate = 16 μg C g^{-1} h^{-1}: Total area 58.96 (44.88%)
27 Warm conifer (0.38)
28 Tropical montane (1.17)
29 Tropical seasonal forest (6.06)
40 Grass/shrub—cool (3.84)
43 Savanna (6.68)
46 Mediterranean (0.91)
47 Dry highland (2.51)
50 Sand desert (5.26)
51 Semidesert (7.59)
52 Shrub/steppe (1.86)
53 Tundra (8.77)
55 Crop/woods—cool (1.28)
59 Thorn woods (3.90)
Other woods (2.25)
Other desert (4.67)
Other landscapes (1.83)
Emission rate = 24 μg C g^{-1} h^{-1}: Total area 28.59 (21.76%)
24 Temperate mixed (1.95)
33 Tropical rainforest (4.33)
41 Grass/shrub—hot (17.24)
56 Regrowing woods (2.94)
57 Woods—cool (2.13)
Emission rate = 45 μg C g^{-1} h^{-1}: Total area 8.08 (6.15%)
26 Temperate deciduous (0.71)
25 Snowy deciduous (0.74)
32 Drought deciduous (4.6)
48 Dry evergreen (0.91)
60 Dry taiga (1.13)

of water vapor (g_C) versus the quantity (FPAR divided by the canopy extinction coefficient for PAR, k). This simple empirical relationship makes it possible to derive accurate satellite remote sensing estimates of the area-integrals for canopy energy and carbon fluxes, even for spatially heterogeneous vegetation covers.

3. Results and interpretation

3.1. Prediction of global emissions

We estimate an annual global isoprene flux of 559 Tg C using the NASA-CASA model (Fig. 3a). Our global estimated flux is somewhat higher than the predicted emission flux of 503 Tg C yr^{-1} in the earlier study by Guenther et al. (1995) (Fig. 3b). Differences in land cover classification as well as in estimated land mass between various ecosystem maps used in the two studies make the comparisons among isoprene estimates problematic. It is useful, nonetheless, to compare emission rate averages among ecosystem cover types from the DeFries et al. (1994) classification scheme (Table 2). Strong similarities exist between the two model results, ours and those of Guenther et al. (1995), with forest and woodland ecosystems being the largest sources of isoprene emissions. In our model results, three ecosystem cover types, broadleaf evergreen forest, dry tropical forest, and wooded grassland (savanna), are responsible for approximately 80% of global total isoprene emissions from terrestrial vegetation. From global mean values, we estimate almost 50% higher emission rate averages for dry tropical forest and broadleaf deciduous forest than Guenther et al. (1995). Conversely, we estimate almost 50% lower emission rate averages for coniferous evergreen forest, grasslands, and cultivated lands compared to rates averages from Guenther et al. (1995) for these vegetation classes.

Generally speaking, potential differences between the global distributions of terrestrial trace gas fluxes are mainly due to differences in land cover classification, associated base emission rates, and climate/ecosystem interactions. Our estimated biogenic emissions of isoprene are highest in the tropics and lowest in the polar regions. Both moist evergreen tropical forest and dry (drought-deciduous) tropical forest regions show fairly high rates of emission in all months (Fig. 4a and b), although there is substantial variation in isoprene emissions between seasons of the year, related in part to differences in monthly rainfall patterns and seasonal changes in foliar density between the two tropical forest types. Differences between our model predictions and those of Guenther et al. (1995) can be seen clearly in the higher rates of isoprene emission predicted by the NASA-CASA model for evergreen tropical forest and lower seasonal variability in rates for the dry drought-deciduous tropical forest. It appears that differences in estimated seasonal changes in estimated foliar density can explain these model–model differences in isoprene emission rates to a large degree.

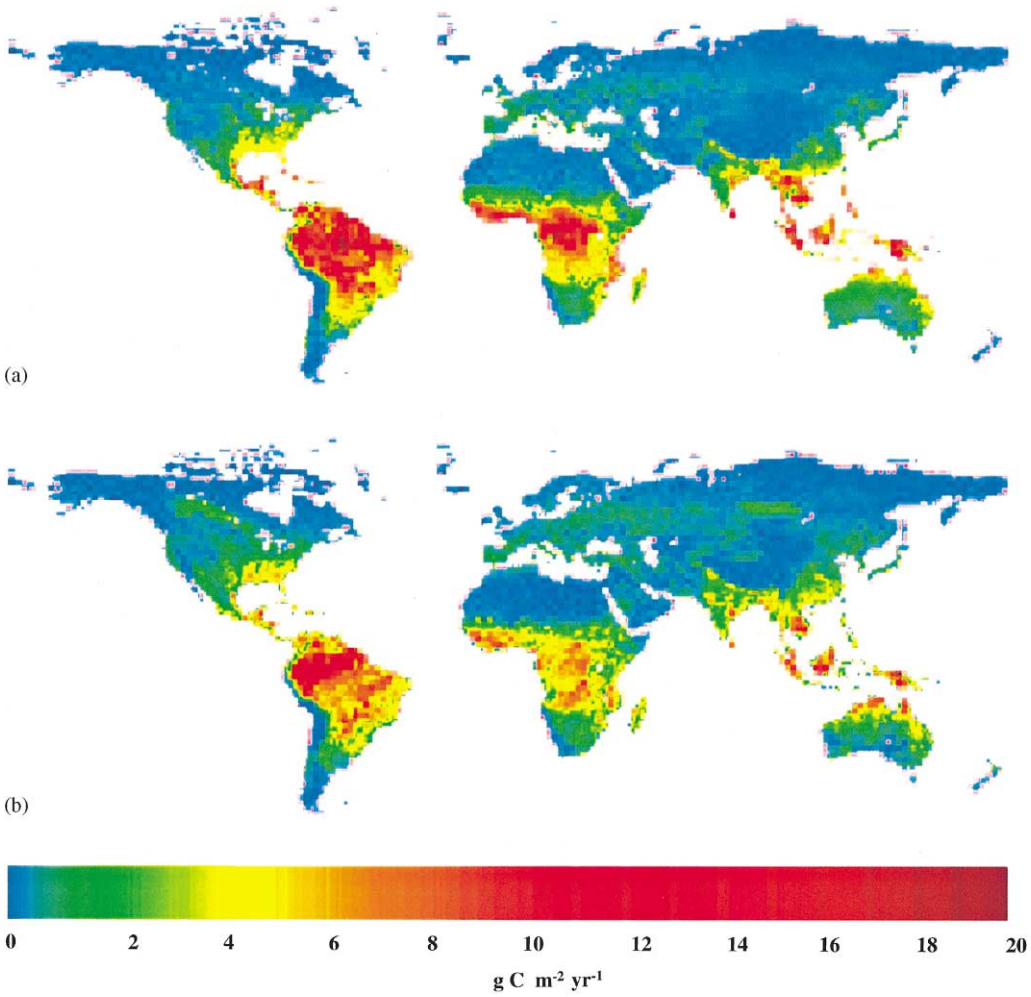

Fig. 3. Global annual emission rates for isoprene from terrestrial vegetation, (a) NASA-CASA model (b) Guenther et al. (1995).

In the temperate and high latitude zones dominated by coniferous forests, emissions vary over the seasons by several orders of magnitude due to high winter–summer fluctuations in temperature and solar radiation (Fig. 4c and d). Emissions peak during the warmest months when leaf temperatures and canopy radiation fluxes are highest. At the temperate coniferous forest site selected for comparison, the model predictions of Guenther et al. (1995) are notably higher than ours during the late summer and fall months (August–October), for reasons that we cannot readily explain.

3.2. Analysis of controllers

In order to better understand the relative influence of climatic (e.g., light and temperature) versus biotic (NPP) controllers on predicted isoprene emission estimates, we generated a series of scatter plots to illustrate the distribution of model 1° grid cell results on two axes of limitation for potential VOC emission (Figs. 5 and 6). For example, when the terms $f(Q)$ and $f(T)$, as estimated from Eq. (2), are plotted against one another as x-axis and y-axis, respectively (Fig. 5), grid cell estimates falling mainly in the upper-left most section of the plot indicate relatively low temperature limitation, but consistently high light limitation for VOC emissions, according to the global model results. Conversely, grid cells falling mainly in the lower-right most section of the plot indicate relatively low light limitation, but consistently high temperature limitation for VOC emissions. Depending on the clustering pattern of grid cell estimates according to either controller variable, a diffuse cloud of grid points over a wide section of the scatter plot would indicate relatively high variability

Table 2
Predicted emission estimates for isoprene generated by the NASA-CASA Model

No.	Ecosystem type DeFries et al. (1994)	Base emission rate (ε_v) ($\mu g\ C\ g^{-1}\ h^{-1}$)	Average emission[a] ($g\ C\ m^{-2}\ yr^{-1}$)	Land area (km^2)	Global total emission ($Tg\ C\ yr^{-1}$)
1	Broadleaf evergreen forest	24	14.41 (13.7)	9.2×10^6	132.0
2	Coniferous evergreen forest	8	0.38 (0.62)	1.3×10^7	4.8
3	High latitude deciduous woodland	8	0.34 (0.45)	5.7×10^6	2.0
4	Tundra	16	0.06 (0.10)	7.0×10^6	0.4
5	Mixed deciduous/evergreen forest	16	2.26 (2.29)	6.6×10^6	14.9
6	Wooded grassland and savanna	24	9.33 (7.25)	2.2×10^7	202.5
7	Temperate grassland	16	1.69 (2.19)	2.1×10^7	34.7
8	Bare ground	16	0.30 (0.36)	1.7×10^7	5.0
10	Cultivated	5	1.03 (2.50)	1.3×10^7	13.5
11	Broadleaf deciduous forest	45	7.12 (4.02)	2.9×10^6	20.9
13	Shrubs and bare ground	16	1.27 (1.15)	1.1×10^7	14.0
14	Dry tropical forest	45	24.66 (11.71)	4.7×10^6	114.7

[a] Average emission rates in parentheses are estimated from data provided by Guenther et al. (1995), overlayed on the DeFries et al. (1994) ecosystem cover distributions.

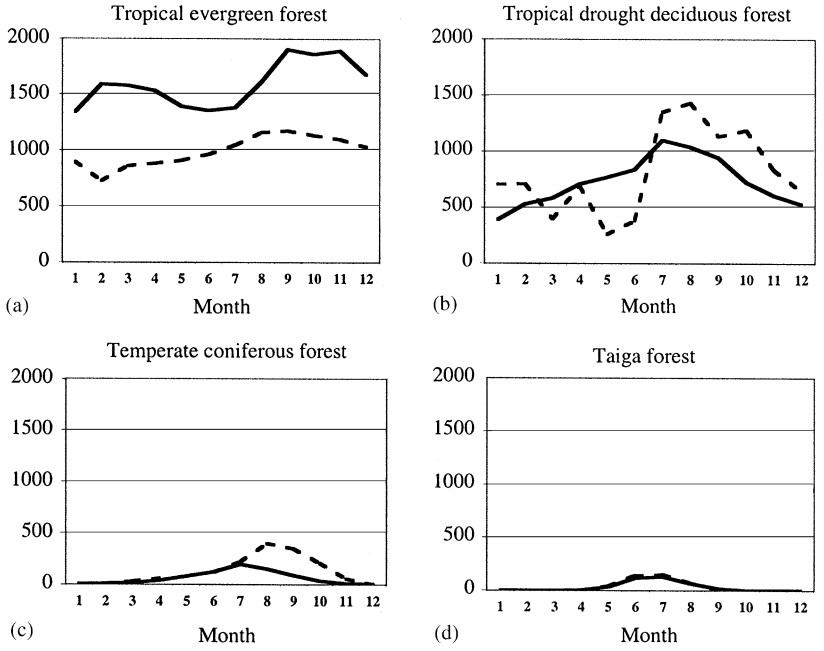

Fig. 4. Model predictions for monthly summed isoprene emissions at four selected forest sites. (a) Manaus, Brazil, (b) Chamela, Mexico, (c) Thompson, OR USA, (d) Bonanza Creek, AK USA. Solid lines are NASA-CASA model, dashed lines from Guenther et al. (1995). Units are $mg\ C\ m^{-2}\ mo^{-1}$.

among grid cell results in terms of both $f(Q)$ and $f(T)$ limitations on VOC emissions. A fairly tightly linear clustering of points extending predominantly along the direction of one axis or the other axis would indicate relatively high variability in either $f(Q)$ or $f(T)$ limitations on VOC emissions, but not in both $f(Q)$ and $f(T)$ limitation terms. Clustering of most points along the 1 : 1 line of the scatter plots would indicate equal levels of limitation on gas emission, with values clustered near 1.0 indicating low limitation potential by both $f(Q)$ and $f(T)$ terms. A majority of points clustered around zero would indicate almost complete limitation

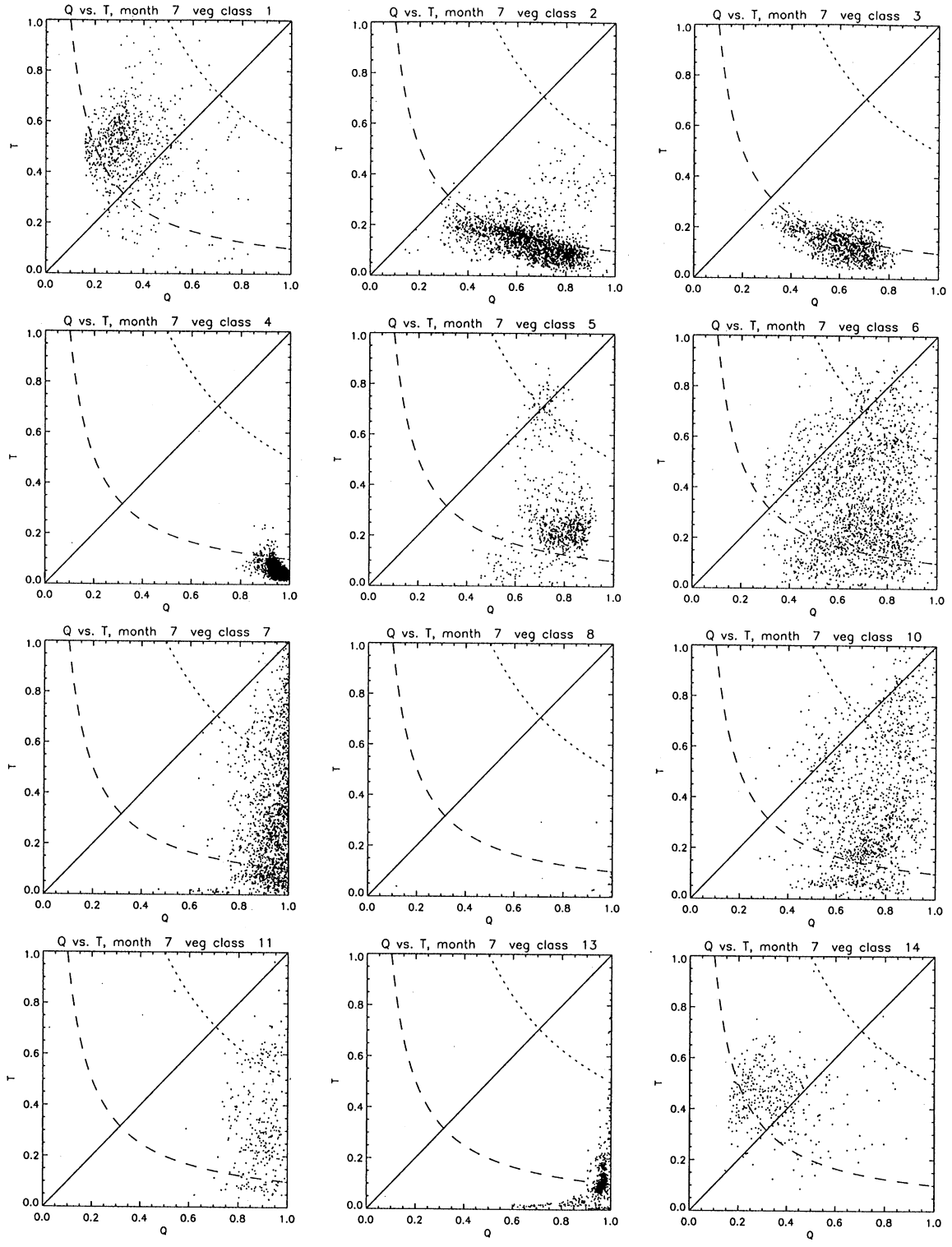

Fig. 5. Scatterplot of T versus Q limiting factors for each ecosystem vegetation type in the classification system of DeFries et al. (1994). Axis product isolines for 0.1 (dashed) and 0.5 (dotted) limitation levels are shown. Vegetation class definitions are: 1 Broadleaf evergreen forest, 2 Coniferous evergreen forest, 3 High latitude deciduous woodland, 4 Tundra, 5 Mixed deciduous/evergreen forest, 6 Wooded grassland and savanna, 7 Temperate grassland, 8 Bare ground, 10 Cultivated, 11 Broadleaf deciduous forest, 13 Shrubs and bare ground, 14 Dry tropical forest.

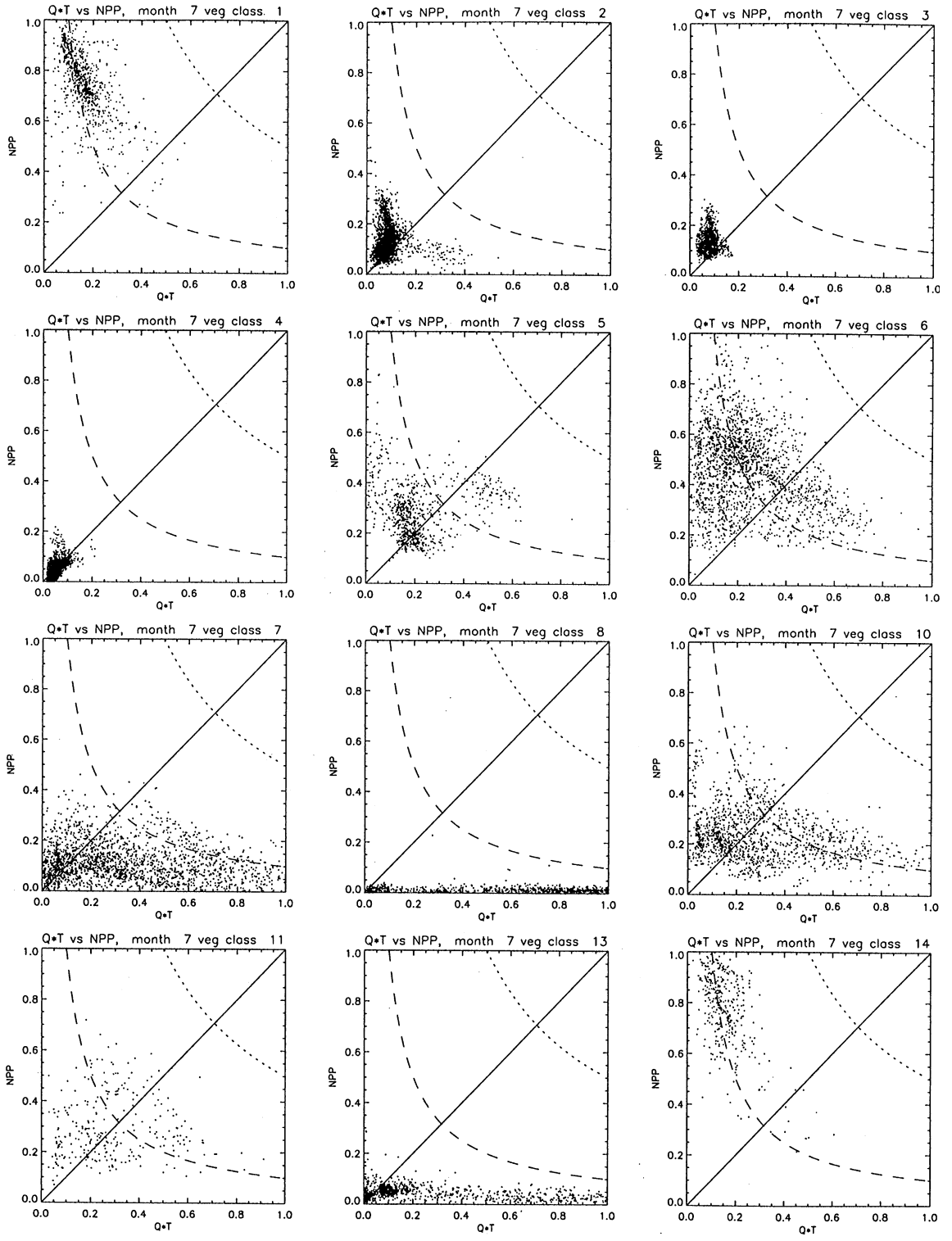

Fig. 6. Scatterplot of biotic (NPP) versus combined climatic ($Q \times T$) limiting factors for each ecosystem vegetation type in the classification system of DeFries et al. (1994). Axis product isolines for 0.1 (dashed) and 0.5 (dotted) limitation levels are shown. Vegetation class definitions are: 1 Broadleaf evergreen forest, 2 Coniferous evergreen forest, 3 High latitude deciduous woodland, 4 Tundra, 5 Mixed deciduous/evergreen forest, 6 Wooded grassland and savanna, 7 Temperate grassland, 8 Bare ground, 10 Cultivated, 11 Broadleaf deciduous forest, 13 Shrubs and bare ground, 14 Dry tropical forest.

of VOC emission rates by a combination of both limitation terms.

Results are presented here only for the month of July, but are generally representative of the year as a whole. Isolines connecting the axis product limitation levels of 0.1 and 0.5 (compared to the non-limited base emission rate level of 1.0) are shown on each plot. For instance, any point falling below the 0.1 isoline is an order of magnitude lower than the non-limited base emission rate for that corresponding grid cell. Plots of $f(T)$ versus $f(Q)$ for each ecosystem type in the classification system of DeFries et al. (1994) indicate that most terrestrial ecosystem types are limited in terms of isoprene emissions by temperature effects (Fig. 5). The limiting temperature effect is readily evident in the plots of high latitude (boreal) forest (classes 2, 3) and tundra ecosystems (class 4), as well as for sub-tropical dry shrubland ecosystems (class 13). Nevertheless, there appears to be substantial variability in light limitation among grid points from the boreal forest classes, which may indicate the effect of heavy cloud cover at many locations during the summer growing season. In contrast, there appears to be substantial variability in temperature limitation effects among grid points from the grassland ecosystem areas (class 7), which are generally predicted to be scarcely light-limited for VOC emissions. Tropical forest ecosystems (classes 1 and 14) appear, on the other extreme, to be mainly light-limited for isoprene emissions, presumably from heavy cloud cover associated with regular daily rainfall patterns. Savanna and cultivated ecosystems (classes 6 and 10) are estimated to be the least limited by combined effects of temperature and light in the model (with the most points falling above the 0.1 and 0.5 isolines), and while highly variable compared to most other classes, are notably less light-limited than predicted for tropical forest ecosystems.

A second series of scatter plots shows the comparison of potential biotic (NPP) versus combined climatic ($Q \times T$) limitations on predicted VOC emissions (Fig. 6). Our remote sensing-based NPP data set is used in this analysis as an indicator of ecosystem carbon cycling rates as organic substrate for VOC emissions. The monthly NPP for July, as predicted by NASA-CASA model, was turned into a 0–1 scalar variable by normalizing to the highest NPP value for July predicted within a given vegetation class. Our VOC model predicts that tropical forest (classes 1 and 14) and savanna (class 6) ecosystems are not strongly limited by biotic controls, but rather by climatic controls on isoprene emissions (i.e., light limitations). These three classes show a substantial number of points with overall emission

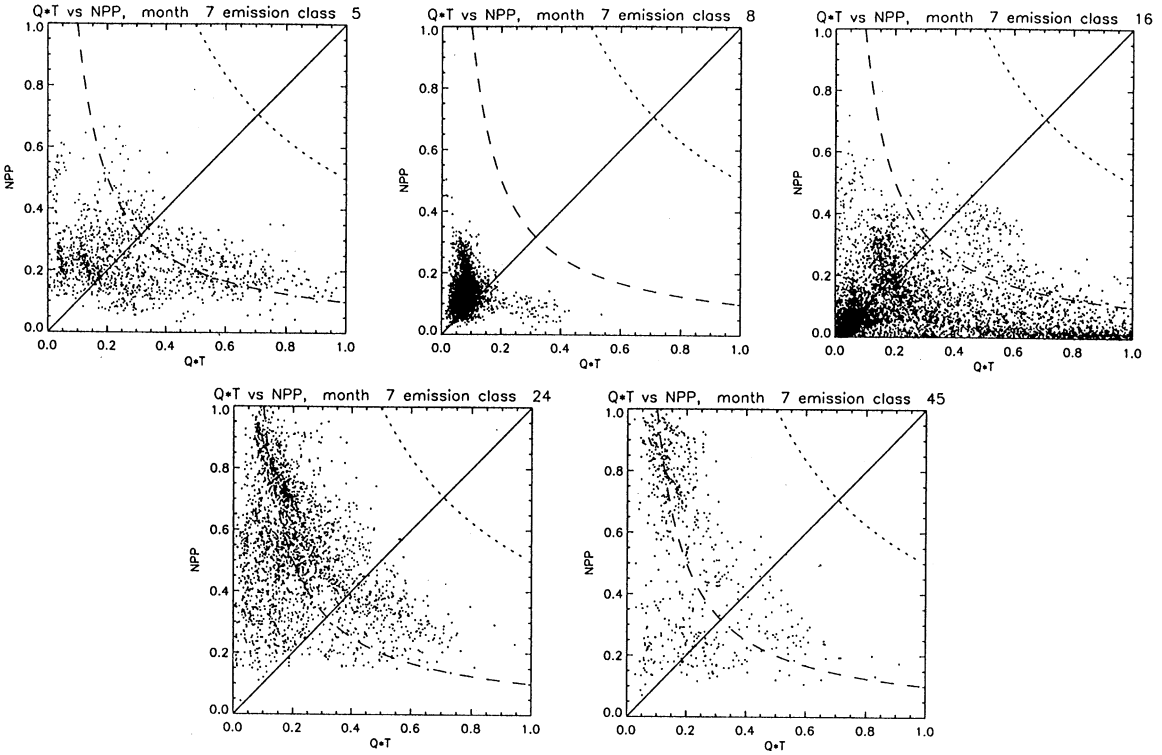

Fig. 7. Scatterplot of biotic (NPP) versus combined climatic ($Q \times T$) limiting factors for each base emission factor class used in the NASA-CASA model for VOC emissions. Axis product isolines for 0.1 (dashed) and 0.5 (dotted) limitation levels are shown.

limitations exceeding 10% (0.1 isoline) of their potential base emission rate. Most other classes are predicted to be limited to well less than 10% (0.1 isoline) of their potential base emission rate. Isoprene emissions are about equally limited by biotic and climatic controls in these cases. Notable exceptions are the desert (class 8) and dry shrubland (class 13) ecosystems, which are mainly limited by biotic effects that manifest in low foliar cover and low potential plant fixation of carbon.

We used this scatter plot approach to further examine the relative importance of base emission factors (ε_v) for isoprene flux in our global model predictions. The estimated biotic (NPP) limitation factor versus the combined climatic ($Q \times T$) limitation factors were (re)grouped according to ε_v classes (Fig. 7) instead of by ecosystem classes (Figs. 5 and 6). It is apparent that there are proportionally low numbers of grid cells in Fig. 7 for which for the overall NPP $\times Q \times T$ limitation effect exceeds 10% (as shown by the 0.1 isolines). This means that, owing to strong limiting factors, base emission rates are rarely expressed globally at levels close to their full potential value in the model calculations. It is worth noting, nonetheless, that the two highest value classes for ε_v (24 and 45 μg C g^{-1} h^{-1}) show the greatest proportion of grid cells with moderate overall limitation effects [(NPP $\times Q \times T$) > 0.1], and also show the highest NPP values, which generally relates to high foliar biomass to support VOC emissions. This pattern implies that base emission factor values remain important determinants of isoprene emissions in the global model formulation, and that ε_v should be treated as a variable to which the global VOC flux estimate can be highly sensitive.

4. Conclusions and future research directions

4.1. Needs for global emissions modeling

The isoprene emission estimates described in this modeling study represent a crucial first step in tightly linking an isoprene flux model to a global ecosystem production model using satellite observations of vegetation cover. Our preliminary work has suggested that land cover classification and associated base emission rates are important controls of isoprene emission rate estimates from models. The differences between annual isoprene emission rate estimates from this study and the results from the Guenther et al. (1995) model arise mostly from differences in ecosystem classification and associated base emission rate categories for isoprene.

By using ecosystem cover types mapped from satellite remote sensing data (DeFries et al., 1994), we have simplified the number of cover types over that of other global isoprene emission models, while incorporating a dynamic classification scheme that should allow inputs of updated satellite observations for land cover and land use change to drive possible future changes in VOC emissions. As the consequence of more accurate land cover classification and between-type discrimination of vegetation forms, overall variance in biogenic emissions estimates within ecosystem cover types should be attributable mainly to variation in local climate factors.

Despite possible advances in trace gas emission fluxes using satellite observations of land surface properties and modeling plant CO_2 fixation rates, large uncertainties may still exist in global VOC emission estimates. In addition to improving the accuracy of mapping various forest vegetation types and foliar densities, improvements in both VOC base emission factors, canopy reentrainment processes, and better understanding of the influence of climate drivers are necessary. For example, while forested regions in tropical ecosystems are the largest source of certain VOCs to the atmosphere, isoprene emission fluxes in these areas are still poorly constrained. Emission algorithms in current VOC global models are based on empirical relationships among light, temperature, and isoprene emission that have been observed mainly in temperate plant studies. Measurements of VOC emissions by Lerdau and Keller (1997) and Lerdau and Throop (1999) have shown that these algorithms may not fit well for many species in tropical forests. A better understanding of the processes controlling VOC emissions in tropical ecosystems will lead to improvements in global model emissions, and offer insight into how VOC emissions from different ecosystems will respond to potential changes in climate. We also note that recent VOC emission studies have suggested that base emission rates at the leaf level of nearly 100 μg C g^{-1} h^{-1} may be realistic for isoprene emissions from temperate forest trees (Guenther et al., 1996; Geron et al., 2000). This is a base emission rate more than two times greater than the highest base emission rate at the ecosystem level specified for our isoprene model (Table 2).

An important lesson from previous VOC emission modeling is that uncertainties in canopy biomass distributions can confound model validation using measurements of gas fluxes. These uncertainties can easily overwhelm any potential advantages of relatively complex models for predicting canopy radiative transfer and photosynthesis rates over simpler model forms (Lamb et al., 1996). From this perspective, potential use of satellite-derived vegetation properties is a critical improvement in moving from leaf to canopy to regional model estimates of biosphere-atmosphere gas and energy exchange. Scaling from leaf to canopy and upward with the aid of remote sensing of ecosystems provides extensive measurements of FPAR, from which canopy modeling parameters related to foliar density can be provided in continuous gridded form. Although the satellite-derived spatial distributions of foliar

biomass density supporting VOC emissions are subject to ground-based validation, previous studies have demonstrated the high quality of such map products for ecosystem carbon cycle models (Sellers et al., 1994; Malmström et al., 1997), even in highly clumped forest canopies (Chen, 1996).

There are additional possibilities for use of remote sensing products in global VOC models. For example, leaf developmental stage, which appears to have a strong limiting effect on VOC emissions during short periods of foliar expansion (Monson et al., 1995), can be tracked by observations of day-to-day 'green-up' rates in the repeated satellite observations of NDVI. Land use changes and forest regrowth patterns may be monitored from satellites as a means of adding spatial and temporal variation in the $f(G)$ term (Eq. (2)) for growth stage effects on canopy VOC emissions.

4.2. Summary of modeling results

While undergoing improvements in light and energy flux controllers for overall carbon metabolism, the NASA-CASA model of isoprene emission fluxes from terrestrial vegetation can reveal a number of important emission patterns operating on scales designed to link regional and global satellite data sets with estimates of ecosystem production, hydrology, and biogeochemistry. Analysis of global drivers, climate control algorithms, and base VOC emission rates in this modeling framework shows that the majority of terrestrial ecosystem classes are limited in terms of isoprene emissions by temperature effects. However, tropical forests (and savanna ecosystems to a somewhat lower degree), which account for a large portion of total biogenic isoprene emitted to the global atmosphere, appear to be most strongly light-limited for these annual VOC emissions. Our model results imply that improvements in global fields of solar surface radiation fluxes must be combined with greater process-level understanding of interactions among light use, foliar temperature, and VOC emissions in warm climate zones in order to reduce major uncertainties in global isoprene source fluxes.

Acknowledgements

This work was supported by a National Research Council Associate Fellowship to Susan Alexander, and by the NASA Earth Observing System Interdisciplinary Science Program, Grant number MDAR-0044-0126, to Christopher Potter, Principal Investigator. We thank Alex Guenther for assistance in model algorithm development.

References

Bishop, J.K.B., Rossow, W.B., 1991. Spatial and temporal variability of global surface solar irradiance. Journal of Geophysical Research 96, 16839–16858.

Bonan, G.B., 1989. A computer model of the solar radiation, soil moisture and soil thermal regimes in boreal forests. Ecological Modelling 45, 275–306.

Box, E., 1981. Foliar biomass: data base of the international biological program and other sources. In: Bufalini, J., Arnts, R. (Eds.), Atmospheric Biogenic Hydrocarbons. Butterworth, Stoneham, Mass.

Chameides, W.L., Lodge, J.P., 1992. Tropospheric ozone: formation and fate. In: Lefohn, A.S. (Ed.), Surface Level Ozone Exposures and their Effects on Vegetation, pp. 1–30. Lewis Pub.

Chen, J.M., 1996. Optically-based methods for measuring seasonal variation in leaf area index of boreal conifer forests. Agriculture and Forest Meteorology 80, 135–163.

Constable, J.V.H., Guenther, A.B., Schimel, D.S., Monson, R.K., 1999. Modeling changes in VOC emission in response to climate change in the continental United States. Global Change Biology 5, 791–806.

DeFries, R., Townshend, J., 1994. NDVI-derived land cover classification at global scales. International Journal of Remote Sensing 15, 3567–3586.

DeFries, R., Field, C., Fung, I., Justice, C., Los, S., Matson, P., Matthews, E., Mooney, H., Potter, C., Prentice, K., Sellers, P., Townshend, J., Ustin, S., Vitousek, P., 1995. Mapping the land surface for global atmosphere–biosphere models: toward continuous distributions of vegetation's functional properties. Journal of Geophysical Research 100, 20867–20882.

Fehsenfeld, F., Calvert, J., Fall, R., Goldan, P., Guenther, A., Hewitt, C., Lamb, B., Liu, S., Trainer, M., Westberg, H., Zimmerman, P., 1992. Emissions of volatile organic compounds from vegetation and the implications for atmospheric chemistry. Global Biogeochemical Cycles 6, 389–430.

Geron, C., Guenther, A., Sharkey, T., Arnts, R., 2000. Temporal variability in basal isoprene emission factor. Tree Physiology 20, 799–805.

Guenther, A., 1999. Modeling biogenic volatile organic compound emissions to the atmosphere. In: Hewitt, C.N. (Ed.), Reactive Hydrocarbons in the Atmosphere. Academic Press, San Diego, pp. 41–94.

Guenther, A., Monson, R.K., Fall, R., 1991. Isoprene and monoterpene emission rate variability: observations with eucalyptus and emission rate algorithm development. Journal of Geophysical Research 96, 10799–10808.

Guenther, A., Hewitt, N., Erikson, D., Fall, R., Geron, C., Graedel, T., Harley, P., Klinger, L., Lerdau, M., McKay, W.A., Pierce, T., Scholes, B., Steinbrecher, R., Tallamraju, R., Taylor, J., Zimmerman, P., 1995. A global model of volatile organic compound emissions. Journal of Geophysical Research 100, 8873–8892.

Guenther, A., Zimmerman, P.R., Klinger, L., Greenberg, J.P., Ennis, C., Davis, K., Pollack, W., Westberg, H., Allwine, G., Geron, C.D., 1996. Estimates of regional natural volatile organic compound fluxes from enclosure and

ambient measurements. Journal of Geophysical Research 101, 1345–1359.

Guenther, A., Baugh, B., Brasseur, G., Greenberg, J., Harley, P., Klinger, L., Serca, D., Vierling, L., 1999. Isoprene emissions estimates and uncertainties for the Central African EXPRESSO study domain. Journal of Geophysical Research 104, 30625–30639.

Holben, B.N., 1986. Characteristics of maximum-value composite images from temporal AVHRR data. International Journal of Remote Sensing 7, 1417–1434.

Iqbal, M., 1983. An Introduction to Solar Radiation. Academic Press, San Diego, CA.

Jumikis, A.R., 1966. Thermal Soil Mechanics. Rutgers University Press, New Brunswick, NJ, 267 pp.

Knyazikhin, Y., Martonchik, J.V., Myneni, R.B., Diner, D.J., Running, S., 1998. Synergistic algorithm for estimating vegetation canopy leaf area index and fraction of absorbed photosynthetically active radiation from MODIS and MISR data. Journal of Geophysical Research 103, 32257–32276.

Lamb, B., Pierce, T., Baldocchi, D., Allwine, E., Dilts, S., Westberg, H., Geron, C., Guenther, A., Klinger, L., Harley, P., Zimmerman, P., 1996. Evaluation of forest canopy models for estimating isoprene emissions. Journal of Geophysical Research 101, 22787–22797.

Leemans, R., Cramer, W.P., 1990. The IIASA database for mean monthly values of temperature, precipitation and cloudiness of a global terrestrial grid. WP-41. International Institute for Applied Systems Analysis; Laxenburg Working Paper, IIASA; Laxenberg, Austria.

Lerdau, M.T., Keller, M., 1997. Controls on isoprene emissions from trees in a subtropical dry forest. Plant, Cell, and Environment 20, 569–578.

Lerdau, M.T., Throop, H.L., 1999. Isoprene emission and photosynthesis in a tropical forest canopy: implications for model development. Ecological Applications 9, 1109–1117.

Los, S.O., Justice, C.O., Tucker, C.J., 1994. A global 1×1 NDVI data set for climate studies derived from the GIMMS continental NDVI data. International Journal of Remote Sensing 15, 3493–3518.

Malmström, C.M., Thompson, M.V., Juday, G.P., Los, S.O., Randerson, J.T., Field, C.B., 1997. Interannual variation in global scale net primary production: testing model estimates. Global Biogeochemical Cycles 11, 367–392.

Monson, R., Fall, R., 1989. Isoprene emission from aspen leaves: photorespiration. Plant Physiology 90, 267–274.

Monson, R., Guenther, A.B., Fall, R., 1991. Physiological reality in relation to ecosystem and global level estimates of isoprene emissions. In: Sharkey, T., Holland, E., Mooney, H. (Eds.), Trace Gas Emissions by Plants. Academic Press, San Diego, pp. 185–207.

Monson, R., Lerdau, M., Sharkey, T., Schimel, D., Fall, R., 1995. Biological aspects of constructing biological hydrocarbon emission inventories. Atmospheric Environment 29, 2989–3002.

Monteith, J.L., 1972. Solar radiation and productivity in tropical ecosystems. Journal of Applied Ecology 9, 747–766.

Norman, J., 1982. Simulation of microclimates. In: Hatfield, J.L., Thomason, I.J. (Eds.), Biometeorology in Integrated Pest Management. Academic Press, New York, pp. 65–99.

Olson, J., 1992. World ecosystems (WE1.4). Digital raster data on a 10 minute geographic 1080×2160 grid. In: NOAA National Geophysical Data Center (Eds.), Global ecosystems database, version 1.0 disc A. Boulder, CO.

Potter, C.S., 1997. An ecosystem simulation model for methane production and emission from wetlands. Global Biogeochemical Cycles 11, 495–506.

Potter, C.S., Randerson, J.T., Field, C.B., Matson, P.A., Vitousek, P.M., Mooney, H.A., Klooster, S.A., 1993. Terrestrial ecosystem production: a process model based on global satellite and surface data. Global Biogeochemical Cycles 7 (4), 811–841.

Potter, C.S., Davidson, E.A., Klooster, S.A., Nepstad, D.C., de Negreiros, G.H., Brooks, V., 1998. Regional application of an ecosystem production model for studies of biogeochemistry in Brazilian Amazonia. Global Change Biology 4 (3), 315–334.

Potter, C.S., Klooster, S.A., Brooks, V., 1999. Interannual variability in terrestrial net primary production: exploration of trends and controls on regional to global scales. Ecosystems 2 (1), 36–48.

Rasmussen, R., Khalil, M., 1988. Isoprene over the Amazon basin. Journal of Geophysical Research 93, 1417–1421.

Running, S.W., Nemani, R.R., 1988. Relating seasonal patterns of the AVHRR vegetation index to simulated photosynthesis and transpiration of forests in different climates. Remote Sensing of Environment 24, 347–367.

Sellers, P.J., Tucker, C.J., Collatz, G.J., Los, S.O., Justice, C.O., Dazlich, D.A., Randall, D.A., 1994. A global 1×1 NDVI data set for climate studies. Part 2: the generation of global fields of terrestrial biophysical parameters from the NDVI. International Journal of Remote Sensing 15, 3519–3545.

Sellers, P.J., Berry, J.A., Collatz, G.J., Field, C.B., Hall, F.G., 1995. Canopy reflectance, photosynthesis, and transpiration. III. A reanalysis using improved leaf models and a new canopy integration scheme. Remote Sensing of Environment 42, 187–216.

Sharkey, T.D., Loreto, E., Delwiche, C., 1991. The biochemistry of isoprene emissions from leaves.. In: Sharkey, T., Holland, E., Mooney, H. (Eds.), Trace Gas Emissions by Plants.. Academic Press, San Diego, pp. 153–184.

Sharkey, T.D., Singsaas, E.L., 1995. Why plants emit isoprene. Nature 374, 769.

Sharkey, T.D., Singsaas, E.L., Lerdau, M.T., Geron, C., 1999. Weather effects on isoprene emission capacity and application of emission algorithms. Ecological Applications 9, 1132–1137.

Singsaas, E.L., Sharkey, T.D., 2000. The effects of high temperature on isoprene synthesis in oak leaves. Plant and Cell Environment 23, 751–757.

Thornthwaite, C.W., 1948. An approach toward rational classification of climate. Geographical Review 38, 55–94.

Turner, D.P., Baglio, J.V., Wones, A.G., Pross, D., Vong, R., McVeety, B.D., Phillips, D.L., 1991. Climate change and isoprene emissions from vegetation. Chemosphere 23, 37–56.

Zimmer, W., Bruggemann, N., Emeis, S., Giersch, C., Lehning, A., Steinbrecher, R., Schnitzler, J.-P., 2000. Process-based modelling of isoprene emission by oak leaves. Plant and Cell Environment 23, 585–595.